



Open Archive TOULOUSE Archive Ouverte (OATAO)

OATAO is an open access repository that collects the work of Toulouse researchers and makes it freely available over the web where possible.

This is an author-deposited version published in : <http://oatao.univ-toulouse.fr/>
Eprints ID : 18550

To link to this article : DOI:10.1016/j.diii.2016.02.011
URL : <https://doi.org/10.1016/j.diii.2016.02.011>

To cite this version : Faruch-Bilfeld, Marie and Lapègue, Franck and Brun, Caroline and Bakouche, Sarah and Cambon, Zoé and Brucher, Nicolas and Chiavassa-Gandois, Hélène and Larbi, Ahmed and Sans, Nicolas *Bone abnormalities of the knee: MRI features.* (2016) Diagnostic and Interventional Imaging, vol. 97 (n° 7-8). pp. 779-788. ISSN 2211-5684

Any correspondence concerning this service should be sent to the repository administrator: staff-oatao@listes-diff.inp-toulouse.fr

Bone abnormalities of the knee: MRI features

M. Faruch Bilfeld^{a,*}, F. Lapègue^a, C. Brun^a,
S. Bakouche^a, Z. Cambon^a, N. Brucher^a,
H. Chiavassa Gandois^a, A. Larbi^b, N. Sans^a

^a Service d'imagerie, hôpital Pierre-Paul-Riquet, CHU Purpan, 1, place de Docteur-Baylac, 31059 Toulouse cedex 9, France

^b Service d'imagerie, CHU Couemeau, place du Professeur Robert-Debré, 30029 Nîmes cedex 9, France

KEYWORDS

Knee;
Cancellous bone;
Cortical bone;
Periosteum;
Diagnostic radiology

Abstract The knee is one of the most studied anatomical structures by magnetic resonance imaging (MRI). Bone abnormalities are very frequently detected, whether or not related to the symptoms for which imaging was indicated. The aim of this pictorial study is to review the most commonly observed bone abnormalities of the knee, bearing in mind that the interpretation of MR images should always take into consideration both clinical and laboratory data, as well as the results of conventional X-ray imaging.

The knee is one of the most studied anatomical structures by magnetic resonance imaging (MRI). Bone abnormalities are therefore detected very frequently, whether or not related to the symptoms for which imaging was indicated. We propose to describe the MRI features of these abnormalities based on how they affect the gross anatomy of long bones. Our article is therefore divided into three sections successively describing abnormalities of the trabecular bone, cortical bone, and periosteum. Albeit artificial, this classification is intended to help in the understanding of such knee abnormalities. Joint abnormalities will not be addressed in this review.

* Corresponding author.

E-mail address: mariefaruch@hotmail.com (M. Faruch Bilfeld).

Conditions affecting trabecular bone

Conditions that mainly affect trabecular bone can be further classified into 4 groups based on their MRI features: epiphyseal edema, epiphyseal necrosis, replacement of trabecular bone, and abnormal bony trabeculae.

Epiphyseal edema

Epiphyseal edema is a MRI feature which does not reflect a real histopathological situation [1]; it is not observed with other imaging modalities such as radiography, computed tomography (CT), or ultrasound. On MR images, bone edema is defined by the presence of hypointense infiltration on T1-weighted images and clear high signal intensity on fat-saturated T2-weighted sequences that is enhanced following injection of gadolinium chelates [2]. The edema is not delimited by a radiolucent demarcation line, and the signal abnormalities have unclear contours [3] (Fig. 1). Epiphyseal edema is generally associated with one of the four following underlying situations: bone bruising, subchondral fracture, complex regional pain syndrome and degenerative disease. Epiphyseal edema is a reversible condition; the length of time before *restitutio ad integrum* being variable [4].

Post-traumatic edema

Post-traumatic epiphyseal edema occurs following direct or indirect trauma. It is an important feature because it reflects the related injury mechanism [5,6] (Fig. 2). The intensity of the injury can be evaluated based on the extent of edema (Fig. 3). Spontaneous resorption of the edema is generally observed, with varying time courses reported in the literature before complete disappearance [7,8].

Edema associated with subchondral fractures

Stress fractures occur when the workload placed on the bone is repeatedly greater than the bone can bear. There are two main kinds of stress fracture: fatigue fractures caused by overuse of structurally normal bone, and insufficiency



Figure 1. Post-traumatic epiphyseal edema following knee injury with an anterior cruciate ligament tear. Edema of the anterior portion of the lateral femoral condyle with infiltration observed as a hypointense signal on T1-weighted images (a) and high signal intensity on fat-saturated T2-weighted images (b). The borders of the edema are imprecise and irregular without a clear demarcation line. The edema of the anterior femoral condyle (arrow) is mirrored by an edema of the posterior tibial plateau, which suggests ACL injury due to excessive anterior tibial translation (arrow blue). Note the anterior tilt of the posterior horn of the meniscus (*).

fractures that occur when the bone is weakened, generally in a patients with osteoporosis [9]. Stress fractures occur in the absence of a traumatic event and are localized in 60% of cases on the medial femoral condyle [10]. Recovery from stress fractures is spontaneous [4].

MRI findings are identical for insufficiency fractures and fatigue fractures [11]. Edema is maximal in the subchondral region and decreases gradually towards the metaphysis; it is not delimited by a demarcation line [3]. On T1- and T2-weighted images, linear hypointensities are observed in the zone of impact on the epiphysis [12]. Each fracture line stems from a single point and can occur anywhere on the subchondral bone [3] (Fig. 4).

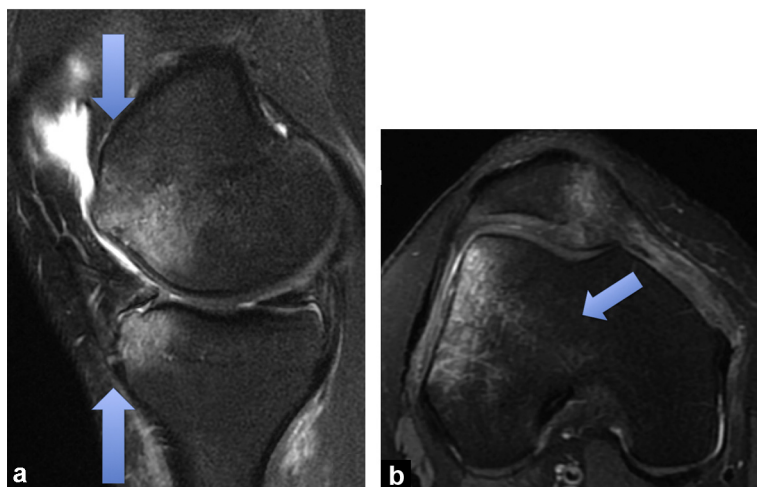


Figure 2. Edema localization and spread reflects the mechanism of injury (arrows): a: mirrored edema pattern in the anterior portions of the femoral condyle and tibial plateau reflecting injury by hyperextension; b: mirrored edema pattern in the medial facet of the patella and the lateral femoral condyle reflecting patellar dislocation.

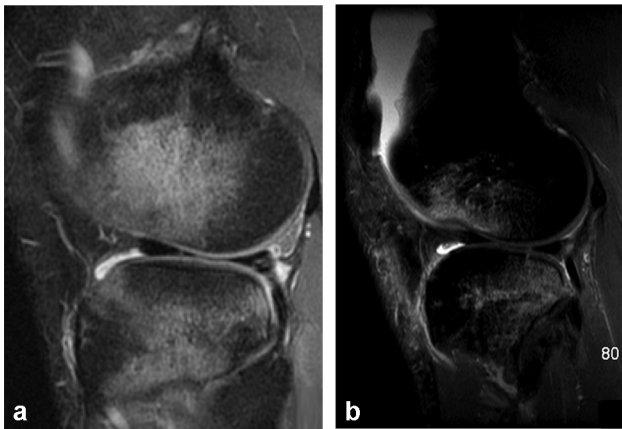


Figure 3. The extent of edema reflects the intensity of injury: a: PD fat-saturated image in the sagittal plane. Mirrored pattern of relatively localized and limited high signal intensity in the anterior femoral condyle and the posterior tibial plateau reflecting low-intensity injury; b: PD fat-saturated image in the sagittal plane. Mirrored pattern of extensive high signal intensity in the anterior femoral condyle and the posterior tibial plateau reflecting high-intensity injury.

Edema associated with type 1 complex regional pain syndrome

Type 1 complex regional pain syndrome (CRPS) is a polymorphic condition of unknown etiology; it is triggered by trauma in only 50% of cases. The main symptom of CRPS is locoregional pain associated with trophic disorders and increased skin sensitivity to touch. No abnormal laboratory values are detected. This syndrome can resolve spontaneously within 6–12 months without sequelae [13]. X-ray and CT scans show disparate increased radiolucency with bone that appears “patchy” mostly in the subchondral region (Fig. 5). However, the appearance of these radiographic features is delayed compared with the onset of symptoms [14]. MR imaging demonstrates the presence of non-specific epiphyseal edema which precedes the bone demineralization observed on radiographs. Partial or diffuse edema may be observed but it is characterized in CRPS by its migration between successive imaging visits [13] (Fig. 6).

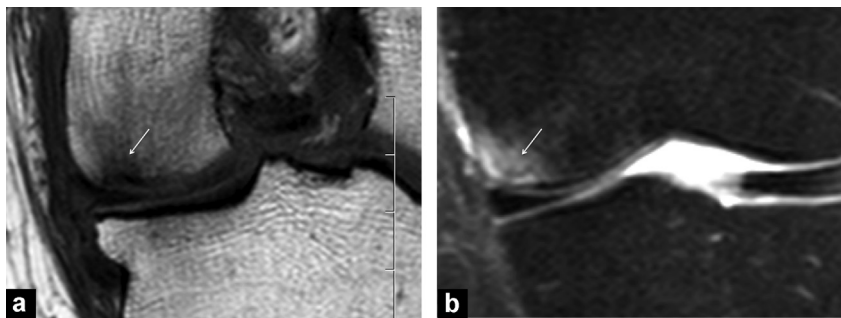


Figure 4. Subchondral fracture of the medial femoral condyle. T1-weighted image (a) and PD fat-suppressed image (b) in the coronal plane. The arrow shows a linear hypo-intensity on both T1- and T2-weighted images stemming from a single subchondral location that reflects impact on the epiphysis.

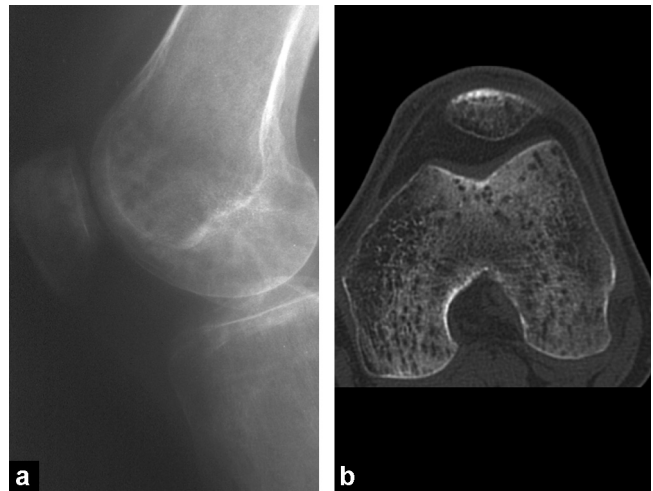


Figure 5. Type 1 complex regional pain syndrome: a: lateral radiograph of the knee reveals “patchy” bone demineralization; b: CT image of the knee in the transverse plane shows heterogeneous demineralization of the distal femoral epiphysis.

Edema associated with cartilage lesions

Epiphyseal edema is often a feature associated with focal or widespread cartilage lesions. In such cases, edema is caused by progressive cartilage damage and is generally symptomatic [15,16] (Fig. 7).

However, it is important to note that not all imaging abnormalities observed in the epiphysis are disease-related. Indeed, in young subjects, red marrow islands may be seen to persist within the metaphysis region and appear as poorly delimited signal abnormalities which are discrete and hyperintense on T2-weighted images and hypointense on T1-weighted images [17] (Fig. 8).

Epiphyseal necrosis

Unlike edema, epiphyseal necrosis causes irreversible damage [18]. Imaging shows a radiolucent demarcation line excluding a zone of abnormal bone. Epiphyseal necrosis occurs in two distinct clinical situations: spontaneous/mechanical osteonecrosis and systemic osteonecrosis.

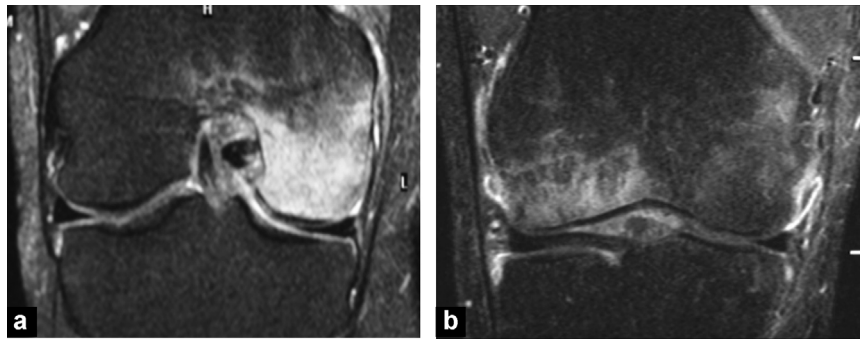


Figure 6. Type 1 complex regional pain syndrome: a: edema of the medial femoral condyle on PD fat-suppressed image in the coronal plane; b: 3 months later, the edema has migrated to the lateral femoral condyle.

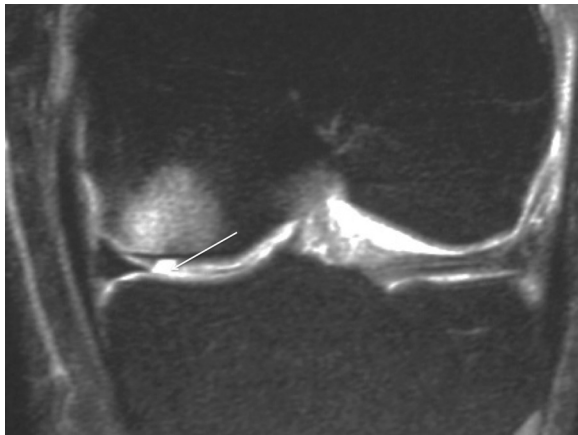


Figure 7. Epiphyseal edema associated with focal cartilaginous ulceration (arrow) of the lateral femoral condyle; PD fat-suppressed image in the coronal plane.

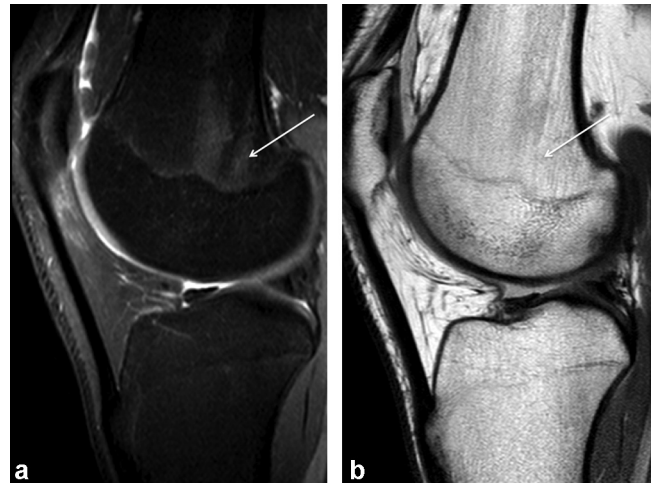


Figure 8. Red marrow islands in the metaphysis region showing slight high signal intensity on the PD fat-suppressed image (a) and hypointensity on the T1-weighted image (b).

Spontaneous osteonecrosis

Spontaneous osteonecrosis is due to repeated stress microfractures that cause ischemia. It is most often observed in elderly subjects within the weight-bearing area of the medial femoral condyle. Patient questioning suggests a sudden onset, without contributing metabolic factors [19].

Radiographic features are often normal in the early stages, then show subchondral abnormalities representing bone collapse: subchondral dissection followed by damage to the articular surface [2] (Fig. 9). Knee MRI shows

epiphyseal edema in the subchondral region that is not delimited by a radiolucent line, combined with fissure lines that make the condition difficult to differentiate from subchondral fracturing [3] (Fig. 10). Spontaneous necrosis is probable when fissures are observed at some distance from subchondral bone, the margins of the epiphysis appear deformed, there are areas of hypointense signal on T2-weighted images (thickness > 4 mm or length > 14 mm), and subchondral bone is not enhanced following gadolinium chelate injection [2,4,20].



Figure 9. Radiographic features of spontaneous necrosis: a: subchondral dissection of the medial femoral condyle (arrow); b: deformed epiphysis margins on the lateral femoral condyle reflecting bone collapse (arrow).

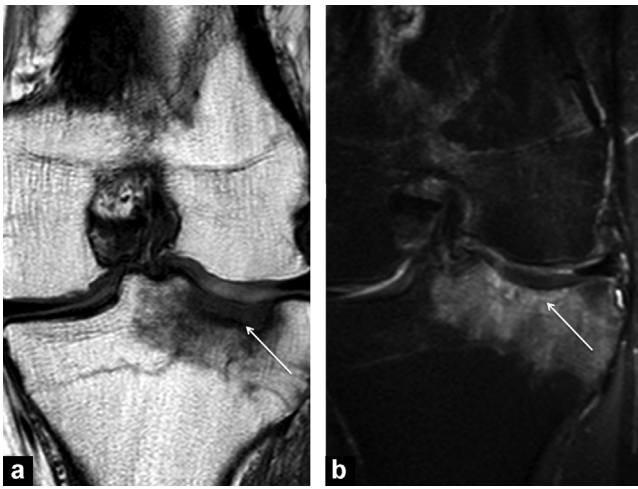


Figure 10. Necrosis of the medial femoral condyle, T1-weighted image (a) and PD fat-suppressed image (b) in the coronal plane. Note the width of the hypointense necrotic fragment (arrow) on the T1-weighted image and the heterogeneous aspect on the PD Fat Sat image.

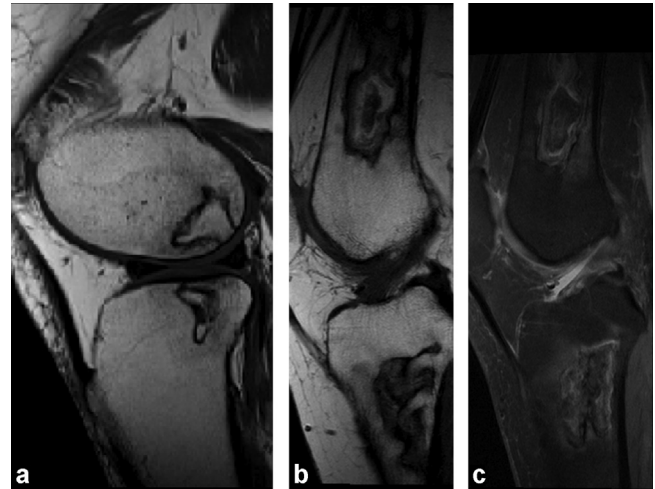


Figure 11. a: systemic osteonecrosis of the epiphysis, T1-weighted image in the sagittal plane; b and c: systemic osteonecrosis of the metaphysis, T1-weighted image (a) and PD fat-suppressed image (b) in the sagittal plane. Note the heterogeneous aspect of the bone tissue within the demarcation line that reflects bone collapse.

Systemic osteonecrosis

The clinical background for systemic osteonecrosis differs from that of spontaneous osteonecrosis because the condition is observed in subjects at risk (alcoholism, sickle cell anemia, hyperuricemia, hypercorticism, etc.). Necrosis is frequently bilateral and observed in the epiphysis or the metaphysis [21].

MRI features are typical with a double line sign (inner hyperintense signal and outer hypointense signal) on T2-weighted images which is thought to be due to a “chemical shift” artifact [18] (Fig. 11). The signal of the zone of necrotic bone can vary, the signs of collapse being inhomogeneous areas on both T2- and T1-weighted images [22]. Using radiography, there is a significant delay between bone infarct onset and development of radiographic features such as calcified infarct and a radiolucent rim [3].

Replacement of cancellous bone

This set of clinical entities is characterized by a localized replacement of normal cancellous bone tissue by another tissue type. They include neoplastic lesions, both benign and malignant, as well as infectious conditions with intraosseous abscess (Figs. 12 and 13). One of the goals of imaging is to determine the nature of the replacement tissue: bony, cartilaginous, liquid, etc. (Fig. 14). In the majority of cases, the border between normal cancellous bone tissue and the replacement tissue are clearly demarcated. However, the imaging features of neoplastic diseases do not always reveal a replacement of cancellous bone. For example, the MRI images of children with leukemia show bone lesions as metaphyseal lucent bands (“leukemia lines”) which seem to be

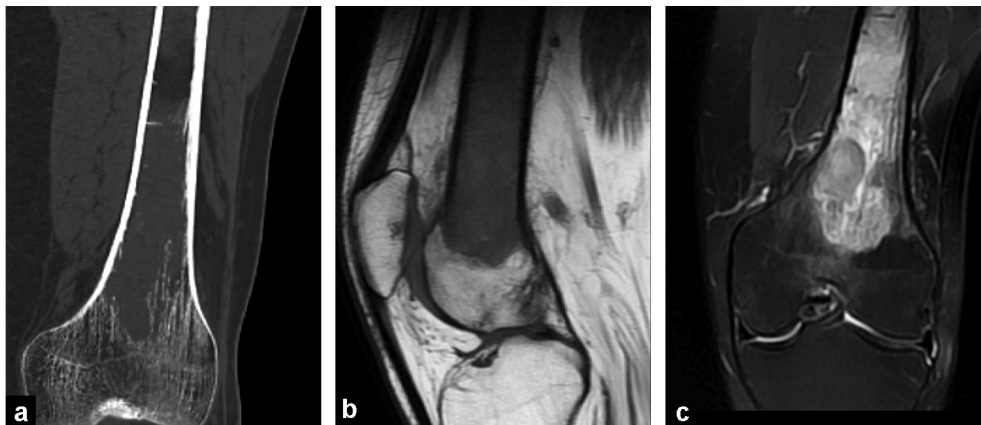


Figure 12. Primary lymphoma of bone: a: CT image in the coronal plane shows medullary invasion with preservation of cortical bone; b, c: MR imaging shows infiltrated tumoral tissue as a hypointense signal on T1-weighted images (b) that enhances following injection of gadolinium chelate (c).

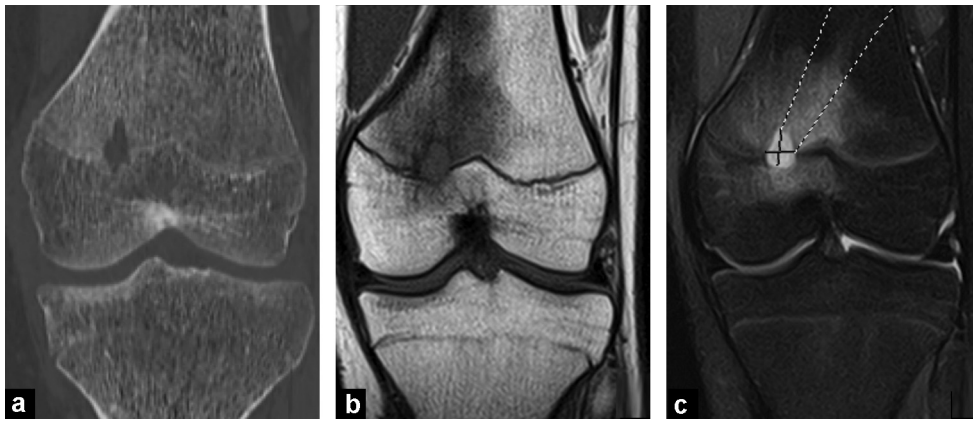


Figure 13. Brodie abscess in the distal femoral metaphysis: a: CT image in the coronal plane shows central osteolysis delimited by a sharp rim; b, c: MR images in the coronal plane show a metaphyseal collection of low signal intensity on T1-weighted images (b) and high signal intensity on STIR images (c).

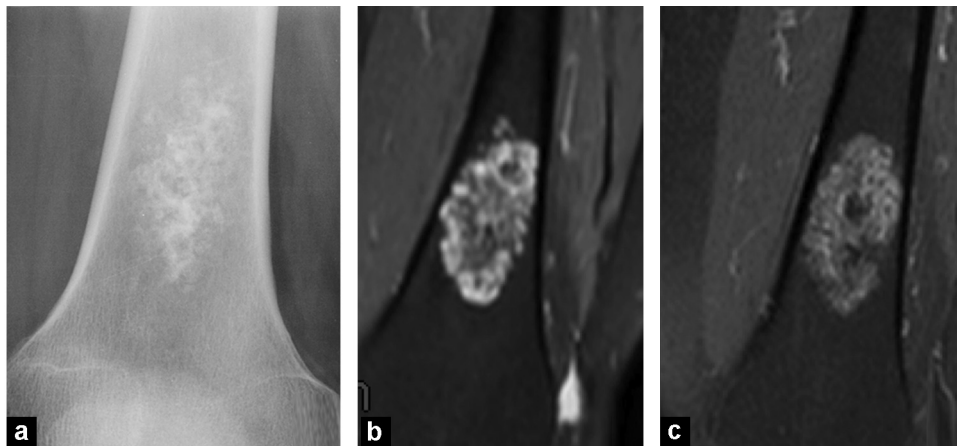


Figure 14. Femoral endochondroma. The cartilaginous nature of the lesion is suspected based on the cartilaginous calcifications observed on CT scan (a), a clear high signal intensity on T2-weighted images (b) and the ring-and-arch pattern with contrast enhancement (c).

due to local changes in the growth of endochondral bone [23] (Fig. 15).

Abnormal bony trabeculae

Changes to the bony trabecular structure are characterized by altered bone architecture related to a metabolic bone disorder. Paget's disease is the most typical example and is characterized by excessive bone remodeling that results in alternating cycles of bone resorption and intensive bone reconstruction [24]. The MRI features of Paget's disease are coarser, sparser and disorganized trabeculae with persisting areas of fat density between the trabeculae, a thickening of cortical bone and deformed and enlarged bones (Fig. 16). Abnormal bony trabeculae are also observed in patients with hemoglobin related diseases and endocrinopathies.

Conditions affecting cortical bone

Cortical bone abnormalities are less frequent than trabecular defects.

Traumatic lesions of cortical bone

Such lesions are evidence of ligament or tendon avulsion [25]. When detected, further investigation can be carried out to determine the related ligament, tendon or meniscal damage [26]. The most typical example of cortical bone damage is the avulsion of the cruciate ligaments from the tibial eminence [27] (Fig. 17). Anterior cruciate ligament avulsion fractures generally occur on hyperextension or hyperflexion of the knee with internal tibial torsion. Such avulsion fractures are frequently associated with injury to the meniscus, internal and external collateral ligaments and posterior cruciate ligament. The Second fracture has

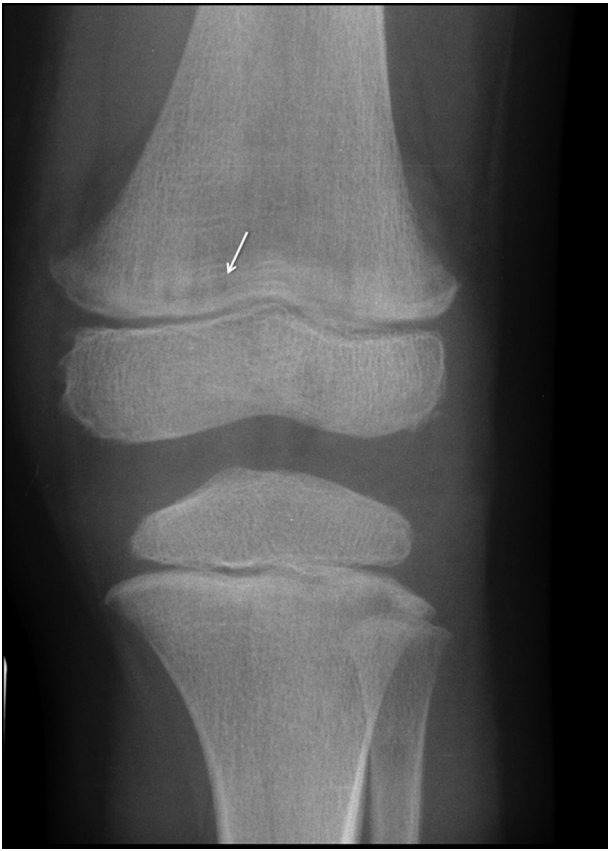


Figure 15. Acute leukemia in a 5-year-old child: clear lucent bands in the metaphysis (arrow).

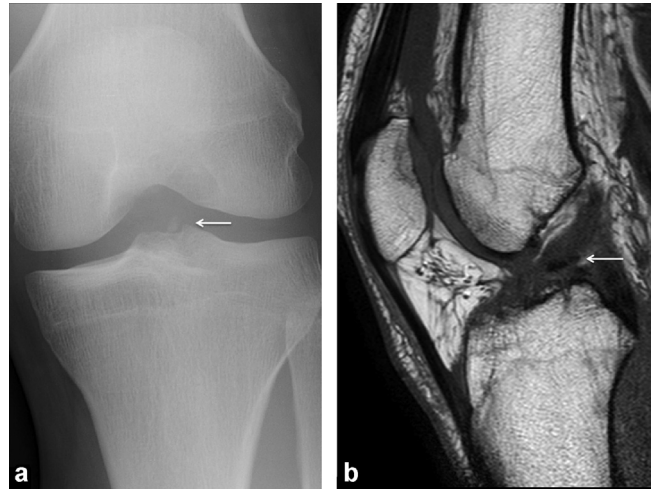


Figure 17. a: avulsion fracture of the anterior tibial eminence on an anteroposterior radiograph; b: T1-weighted MR image in the sagittal plane showing a thickened, loose anterior cruciate ligament attached to the avulsed bone fragment (arrow).

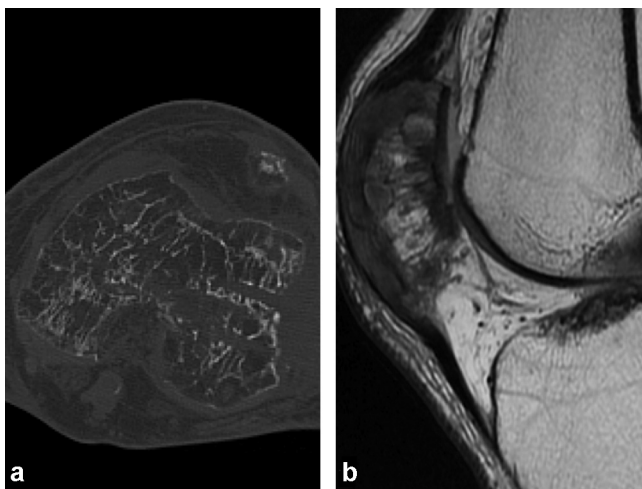


Figure 16. Paget's disease: a: Paget's disease of the distal femur. CT scan showing the thickened, coarser aspect of bony trabeculae and reduced trabecular density; b: Paget's disease of the patella. T1-weighted MR image shows a signal within the bone marrow of fatty density (intense signal on T1-weighted images), with hyper-trophic bony trabeculation.

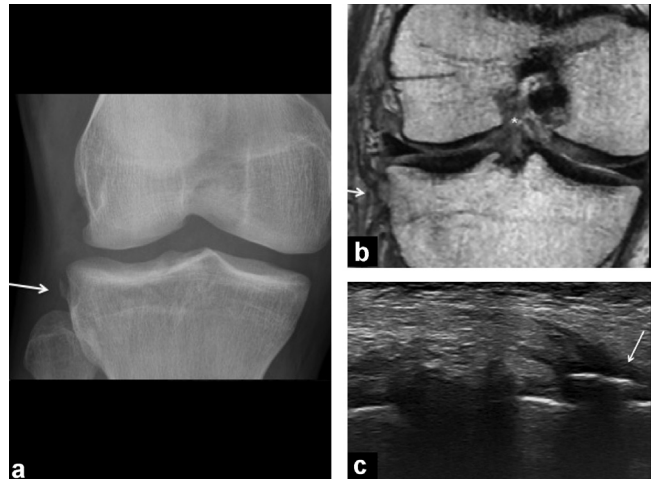


Figure 18. Second fracture: a: anteroposterior radiograph showing avulsion of the lateral tibial plateau (arrow); b, c: PD fat-suppressed MR image in the coronal plane (b) and ultrasound (c) showing the thickened anterolateral ligament attached to the avulsed bone fragment (arrows).

recently aroused interest because related to the anterolateral ligament [28,29]. It is probably an avulsion fracture of the lateral tibial plateau caused by pulling on the anterolateral ligament (Fig. 18). It occurs as a result of internal

rotation and varus stress and is very frequently associated with anterior cruciate ligament injury [30,31].

Tumors of cortical bone

It is important to be able to recognize typical cortical bone lesions.

Osteoid osteoma is a benign tumor seen in children and young adults with typical clinical signs and imaging findings. Patients experience daily pain that increases at night causing insomnia and is generally relieved by aspirin [32]. Radiography and CT scans reveal a lacuna measuring less than 1 cm called a "nidus" that can sometimes contain a central calcification surrounded by a cortical osteosclerotic

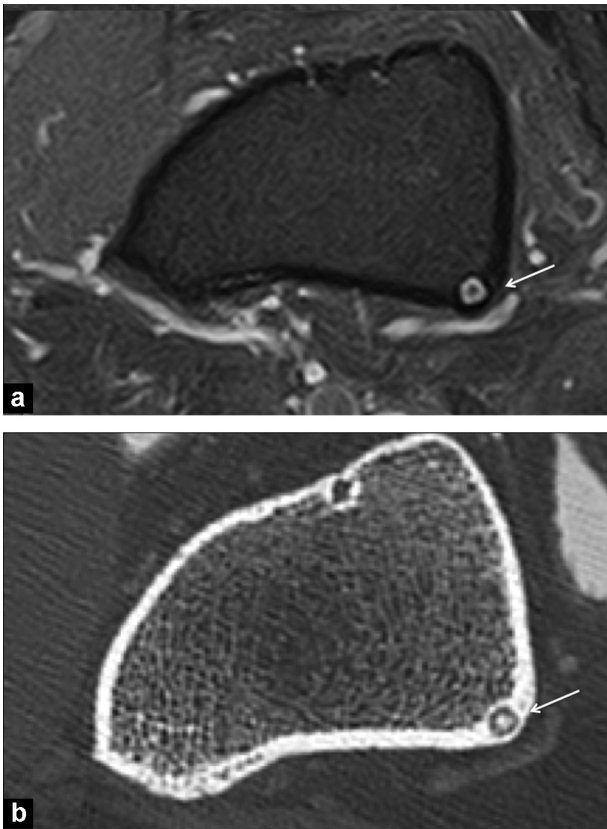


Figure 19. Osteoid osteoma of the tibia: a: CT scan shows a lacuna of the cortex, or “nidus” (arrow); b: the nidus is enhanced (arrow) on fat-saturated T1-weighted images following gadolinium chelate injection.

reaction (Fig. 19). On MR images, the nidus shows up as a hypointense signal on all sequences and is associated with significant edema of the bone and soft tissue. Dynamic gadolinium-enhanced MR imaging shows peak enhancement at the arterial phase with a very fast wash-out [33].

Nonossifying fibroma (NOF) is a benign bone lesion that affects 30–40% of children and adolescents. It is generally asymptomatic and discovered as an incidental finding. NOF can be diagnosed based only on radiographic findings which reveal cortical off-center oval-shaped lacuna with a sharply demarcated rim and a main axis parallel to that of the diaphysis (Fig. 20). Most NOFs require no treatment or monitoring [32].

Conditions affecting the periosteum

The periosteum is membrane covering the outer surface of all bones except at the articular surfaces. It is composed of an inner cellular layer and an outer fibrous layer that enable intramembranous osteogenesis during growth and in adults. Under normal conditions, the periosteum cannot be visualized by imaging. However, some pathological conditions can cause the periosteum to detach from the bone, for example pediatric osteoarticular infections or subperiosteal hematoma [34] (Fig. 21).

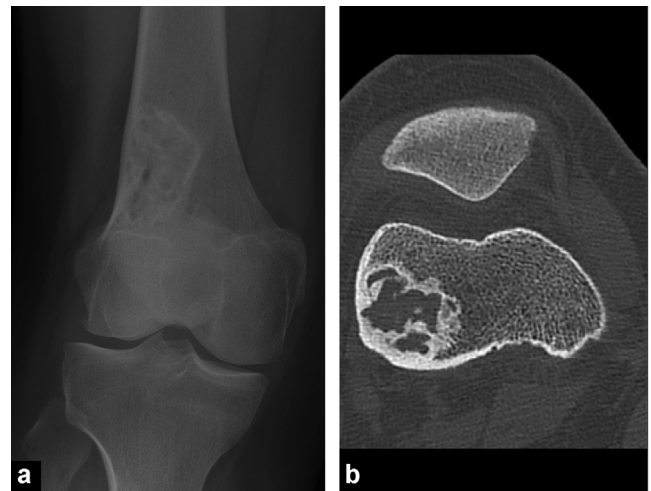


Figure 20. Nonossifying fibroma of the distal femur. Anteroposterior radiograph (a) and CT scan (b) shows an oval-shaped osteolytic lesion of cortical bone, with peripheral osteosclerosis. The lesion main axis is parallel to the axis of the diaphysis.

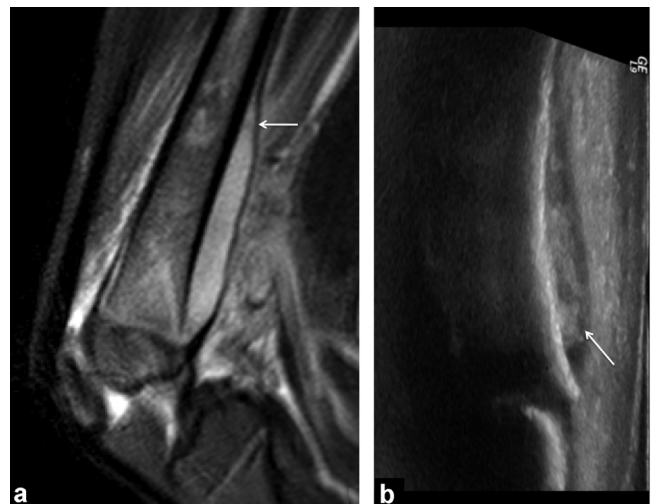


Figure 21. Subperiosteal abscess of the femoral metaphysis: a: STIR-weighted MR image in the sagittal plane showing subperiosteal liquid collection. Note how the periosteum is represented by a hypointense signal (arrow); b: ultrasound imaging showing a hypoechoic collection contiguous to cortical bone.

Periosteal reaction is a non-specific response of the periosteum to aggression by bone formation. The intensity of periosteal reaction depends on the time course of aggression. Continuous periosteal reaction, with or without preservation of the cortical surface, can be distinguished from interrupted periosteal reaction that is indicative of a more aggressive lesion [35]. Periosteal reaction does not necessarily reflect a neoplastic process; long bone hair-line fractures and osteomyelitis can also result in periosteal reaction (Fig. 22).

Take-home messages

- Prior knowledge of a patient's clinical background and laboratory values is important prior to imaging studies of the knee.
- Conventional radiography is still essential. MRI should be used as a second-intention tool for more detailed imaging of the lesions.
- Edema observed on MRI generally precedes abnormal findings using conventional radiography.
- Edema resulting from fatigue fractures or bone weakness is maximal in the subchondral region and decreases gradually towards the metaphysis, but is not demarcated by a radiolucent line. It is associated with linear hypointensities on T1- and T2-weighted images. Unlike osteonecrosis, each fracture line stems from a single point and can occur anywhere on the subchondral bone.
- Findings in favor of spontaneous necrosis: fissures observed at some distance from subchondral bone, the margins of the epiphysis appear deformed, there are areas of hypointense signal on T2-weighted images (thickness > 4 mm or length > 14 mm), and subchondral bone is not enhanced following gadolinium chelate injection.
- The diagnosis of neoplastic, infectious and metabolic diseases also benefits from comparison with conventional imaging and computerized topography.

Clinical case

A 73-year-old woman was referred to you for conventional radiographic imaging focusing on the proximal end of the tibia; her attending physician has detected by palpation an immobile lump on the tibia. Fig. 23a shows a photograph of the patient's legs.

Questions

- 1) Describe the abnormalities seen on the radiograph (Fig. 23b).

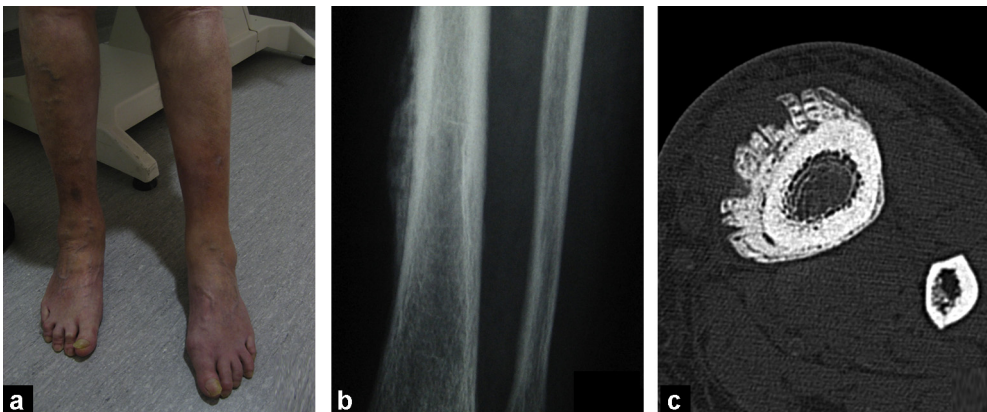


Figure 23. Hard lump on the deep tibia: a: photograph of patient's legs; b: anteroposterior radiograph; c: CT scan without injection of iodinated contrast agent.

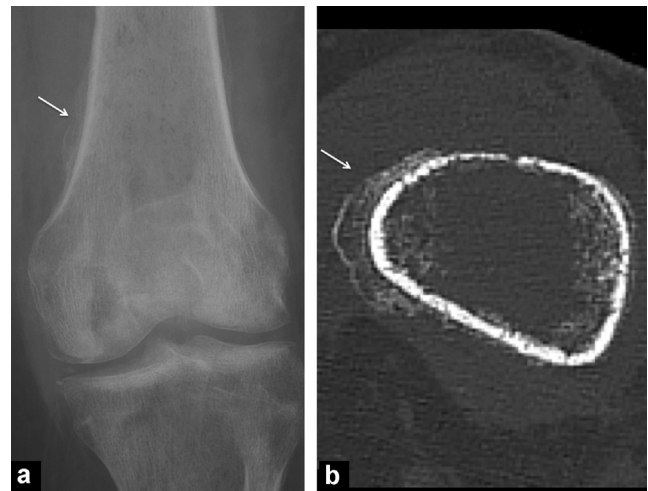


Figure 22. Subacute osteomyelitis of the femur: a: anteroposterior radiograph shows continuous periosteal reaction (arrow); b: CT image in the transverse plane shows osteolysis of moth-eaten appearance and continuous periosteal reaction (arrow).

- 2) The patient underwent a complementary CT scan (Fig. 23c). What abnormalities can be seen?
- 3) What is your diagnosis?

Answers

- 1) The anteroposterior radiograph reveals continuous, although irregular, periosteal reaction. No abnormalities are observed in the adjacent soft tissue. No osteolysis is detected.
- 2) The CT scan confirms the presence of significant periosteal reaction incorporated in the cortex. No abnormalities were detected in the cortical bone or cancellous bone. Dilated veins can be observed in adjacent soft tissue.
- 3) The diagnosis is periosteal reaction related to chronic venous insufficiency [36] (Fig. 23).

Disclosure of interest

The authors declare that they have no competing interest.

References

- [1] Thiryayi WA, Thiryayi SA, Freemont AJ. Histopathological perspective on bone marrow oedema, reactive bone change and haemorrhage. *Eur J Radiol* 2008;67(1):62–7.
- [2] Lecouvet FE, Malghem J, Maldague BE, Vande Berg BC. MR imaging of epiphyseal lesions of the knee: current concepts, challenges, and controversies. *Radiol Clin North Am* 2005;43(4):655–72.
- [3] Malghem J, Lecouvet F, Oumoumi P, Maldague B, Vande Berg B. In: Laredo JD, Wybier M, Petrover D, Morvan G, editors. *Cédèmes transitoires et ostéonécroses du genou. Imagerie rhumatologique et orthopédique. Ceinture pelvienne et membre inférieur*. Montpellier: Sauramps médical; 2013. p. 2226–47.
- [4] Lecouvet FE, van de Berg BC, Maldague BE, Lebon CJ, Jamart J, Saleh M, et al. Early irreversible osteonecrosis versus transient lesions of the femoral condyles: prognostic value of subchondral bone and marrow changes on MR imaging. *AJR Am J Roentgenol* 1998;170(1):71–7.
- [5] Diederichs G, Issever AS, Scheffler S. MR imaging of patellar instability: injury patterns and assessment of risk factors. *Radiographics* 2010;30(4):961–81.
- [6] Robertson PL, Schweitzer ME, Bartolozzi AR, Ugoni A. Anterior cruciate ligament tears: evaluation of multiple signs with MR imaging. *Radiology* 1994;193(3):829–34.
- [7] Vellet D. Magnetic resonance imaging of bone marrow and osteochondral injury. *Magn Reson Imaging Clin N Am* 1994;2(3):413–23.
- [8] Roemer FW, Bohndorf K. Long-term osseous sequelae after acute trauma of the knee joint evaluated by MRI. *Skeletal Radiol* 2002;31(11):615–23.
- [9] Yamamoto T, Bullough PG. Spontaneous osteonecrosis of the knee: the result of subchondral insufficiency fracture. *J Bone Joint Surg Am* 2000;82(6):858–66.
- [10] Yao L, Stanczak J, Boutin RD. Presumptive subarticular stress reactions of the knee: MRI detection and association with meniscal tear patterns. *Skeletal Radiol* 2004;33(5):260–4.
- [11] Viana SL, Machado BB, Mendlovitz PS. MRI of subchondral fractures: a review. *Skeletal Radiol* 2014;43(11):1515–27.
- [12] Gondim Teixeira PA, Balaj C, Marie B, Lecocq S, Louis M, Braun M, et al. Linear signal hyperintensity adjacent to the subchondral bone plate at the knee on T2-weighted fat-saturated sequences: imaging aspects and association with structural lesions. *Skeletal Radiol* 2014;43(11):1589–98.
- [13] Gaeta M, Mazziotti S, Minutoli F, Vinci S, Blandino A. Migrating transient bone marrow edema syndrome of the knee: MRI findings in a new case. *Eur Radiol* 2002;12(Suppl. 3):S40–2.
- [14] Berger CE, Kröner AH, Kristen KH, Grabmeier GF, Kluger R, Minai-Pour MB, et al. Transient bone marrow edema syndrome of the knee: clinical and magnetic resonance imaging results at 5 years after core decompression. *Arthroscopy* 2006;22(8):866–71.
- [15] Link TM, Steinbach LS, Ghosh S, Ries M, Lu Y, Lane N, et al. Osteoarthritis: MR imaging findings in different stages of disease and correlation with clinical findings. *Radiology* 2003;226(2):373–81.
- [16] Phan CM, Link TM, Blumenkrantz G, Dunn TC, Ries MD, Steinbach LS, et al. MR imaging findings in the follow-up of patients with different stages of knee osteoarthritis and the correlation with clinical symptoms. *Eur Radiol* 2006;16(3):608–18.
- [17] Dawson KL, Moore SG, Rowland JM. Age-related marrow changes in the pelvis: MR and anatomic findings. *Radiology* 1992;183(1):47–51.
- [18] Murphey MD, Foreman KL, Klassen-Fischer MK, Fox MG, Chung EM, Kransdorf MJ. From the radiologic pathology archives imaging of osteonecrosis: radiologic-pathologic correlation. *Radiographics* 2014;34(4):1003–28.
- [19] Aglietti P, Insall JN, Buzzi R, Deschamps G. Idiopathic osteonecrosis of the knee. Aetiology, prognosis and treatment. *J Bone Joint Surg Br* 1983;65(5):588–97.
- [20] Björkengren AG, AlRowaih A, Lindstrand A, Wingstrand H, Thorngren KG, Pettersson H. Spontaneous osteonecrosis of the knee: value of MR imaging in determining prognosis. *AJR Am J Roentgenol* 1990;154(2):331–6.
- [21] Mankin HJ. Non-traumatic necrosis of bone (osteonecrosis). *N Engl J Med* 1992;326(22):1473–9.
- [22] Vande Berg BE, Malghem JJ, Labaisse MA, Noel HM, Maldague BE. MR imaging of avascular necrosis and transient marrow edema of the femoral head. *Radiographics* 1993;13(3):501–20.
- [23] Resnick D, Haghighi P. *Lymphoproliferative and myeloproliferative disorders. Diagnosis of bone and joint disorders*. 4^e ed. Philadelphia: Saunders; 2291–345.
- [24] Smith SE, Murphey MD, Motamedi K, Mulligan ME, Resnik CS, Gannon FH. From the archives of the AFIP. Radiologic spectrum of Paget disease of bone and its complications with pathologic correlation. *Radiographics* 2002;22(5):1191–216.
- [25] Venkatasamy A, Ehlinger M, Bierry G. Acute traumatic knee radiographs: beware of lesions of little expression but of great significance. *Diagn Interv Imaging* 2014;95(6):551–60.
- [26] Gottsegen CJ, Eyer BA, White EA, Learch TJ, Forrester D. Avulsion fractures of the knee: imaging findings and clinical significance. *Radiographics* 2008;28(6):1755–70.
- [27] Mellado JM, Ramos A, Salvadó E, Camins A, Calmet J, Saurí A. Avulsion fractures and chronic avulsion injuries of the knee: role of MR imaging. *Eur Radiol* 2002;12(10):2463–73.
- [28] Claes S, Luyckx T, Vereecke E, Bellemans J. The Segond fracture: a bony injury of the anterolateral ligament of the knee. *Arthroscopy* 2014;30(11):1475–82.
- [29] Segond P. *Recherches cliniques et expérimentales sur les épanchements sanguins du genou par entorse* [Internet]. Paris: National Library of France; 1879 <http://www.ncbi.nlm.nih.gov/pubmed>.
- [30] Van der Watt L, Khan M, Rothrauff BB, Ayeni OR, Musahl V, Getgood A, et al. The structure and function of the anterolateral ligament of the knee: a systematic review. *Arthroscopy* 2015;31(3):569–82.
- [31] Pomajzl R, Maerz T, Shams C, Guettler J, Bicos J. A review of the anterolateral ligament of the knee: current knowledge regarding its incidence, anatomy, biomechanics, and surgical dissection. *Arthroscopy* 2015;31(3):583–91.
- [32] Sans N, Perroncel G. *Imagerie des tumeurs osseuses*. Montpellier: Sauramps medical; 2014.
- [33] Liu PT, Chivers FS, Roberts CC, Schultz CJ, Beauchamp CP. Imaging of osteoid osteoma with dynamic gadolinium-enhanced MR imaging. *Radiology* 2003;227(3):691–700.
- [34] Bissere D, Kaci R, Lafage-Proust MH, Alison M, Parlier-Cuau C, Laredo JD, et al. Periosteum: characteristic imaging findings with emphasis on radiologic-pathologic comparisons. *Skeletal Radiol* 2015;44(3):321–38.
- [35] Ragsdale BD, Madewell JE, Sweet DE. Radiologic and pathologic analysis of solitary bone lesions. Part II: periosteal reactions. *Radiol Clin North Am* 1981;19(4):749–83.
- [36] Karasick D, Schweitzer ME, Deely DM. Ulcer osteoma and periosteal reactions to chronic leg ulcers. *AJR Am J Roentgenol* 1997;168(1):155–7.